New Astronomy 77 (2020) 101349

Contents lists available at ScienceDirect

New Astronomy

journal homepage: www.elsevier.com/locate/newast

Study of Exospheric Neutral Composition of Mars observed from Indian Mars Orbiter Mission

Kamsali Nagaraja[a,*], Praveen Kumar Basuvaraj[a], S.C. Chakravarty[a], Praveen Kumar K[b]

[a] Department of Physics, Bangalore University, Bengaluru-560056, India
[b] Indian Space Research Organisation Headquarters, Bengaluru-560231, India

ARTICLE INFO

Keywords:
MOM
MENCA
Mar exosphere
Solar activity

ABSTRACT

The exospheric composition data of Mars for the period 2014–15 has been extracted and analysed using the observations carried out by the MENCA (Mars Exospheric Neutral Composition Analyser) payload on-board the Mars Orbiter Mission (MOM) launched by India. The latitude, longitude, altitude and solar zenith angle coverage of the partial pressure values of different exospheric constituents are determined and assigned to create a new data-set with orbit-wise data assimilation particularly between 260 and 600 km altitude range. Apart from getting the results on mean individual orbits' partial pressure profiles, the variations of the total as well as partial pressures are studied with respect to the distribution of the major atmospheric constituents and their dependence on solar activity. In particular, CO_2 and O variations are considered together for any differential effects due to photolysis and photo-ionisation. The results on the gradual reduction in densities due to decreasing daily mean sunspot numbers and strong response of CO_2 and O pressures to solar energetic particle events like that of 24 December 2014 are presented.

1. Introduction

Early measurements of atmospheric densities and chemical composition close to the surface of Mars were carried out using earth-based remote sensing techniques of high resolution optical spectrometers incorporating the Doppler shift method. These measurements in visible and IR bands indicated CO_2 as the dominant constituent with the total atmospheric pressure of about 6 mb which were later found to be corroborated with the Viking 1 & 2 lander spacecraft results (Moroz, 1998 and references there in). Similarly, from earth-based spectral line measurements, the Martian surface-air concentrations of water vapour (H_2O), molecular oxygen (O_2), carbon monoxide (CO) and isotope ratios of oxygen (O) and Carbon (C) were determined (Barker, 1972; Carleton and Traub, 1972; Kaplan et al., 1969; Young and Young, l977). During the initial years of space exploration, optical spectrometers in UV and IR bands were used in e.g., Mariner 9 orbiter mission resulting in the detection of the hydrogen corona and the confirmation of small densities of ozone in the polar region of Mars (Lane et al., 1973; Barth and Dick, 1974). There were similar observations of lower atmospheric constituents from other spacecraft missions including Mars 3 & 5, Mariner 6 & 7.

While the efforts to measure the atmospheric parameters including the densities of the gaseous constituents near the surface of Mars in the pre-Viking period (i.e., before 1976) have provided some basic information, there was a need to carry out further observations particularly related to the spatial distribution of the atmospheric constituents in the thermosphere and exosphere of Mars. Such an opportunity was provided by the launch of two Viking spacecraft missions during September 1976 to carry out the observations using mass spectrometers both on the entry probe as well as on the lander. The first in-situ data of the Martian upper atmospheric composition, densities and temperatures were obtained from this twin Viking mission (Hanson et al., 1977; Nier and McElroy, 1977; Owen et al., 1977; Hanson and Mantas, 1988). This was followed by Phobos-2 (1989), Mars Global Surveyer (MGS, 1997) and the Mars Express (2004) missions with main emphasis to study the interaction of solar wind charged particles with Mars, global mapping of the magnetic field and estimating escape rates of ions from Mars (Sagdeev and Zakharov, 1989, Acuna et al., 1999; Barabash et al., 2007). The Mars Pathfinder mission (1997) was the first successful lander-rover mission with similar findings as that of Viking (Magalhaes et al., 1999). Mars Odyssey (2002) and Mars Exploration Rovers Spirit and Opportunity (2004) searched for the surface features affected by flow of water and the atmosphere close to the ground (Mangold et al., 2004; Squyres et al., 2006). More recent missions like Mars Reconnaissance Orbiter (MRO, 2006), Phoenix lander (2008) and Mars Science Laboratory (MSL, 2012) revealed hemispherical

* Corresponding author.
E-mail address: kamsalinagaraj@bub.ernet.in (K. Nagaraja).

https://doi.org/10.1016/j.newast.2019.101349
Received 26 July 2019; Received in revised form 9 November 2019; Accepted 20 November 2019
Available online 21 November 2019

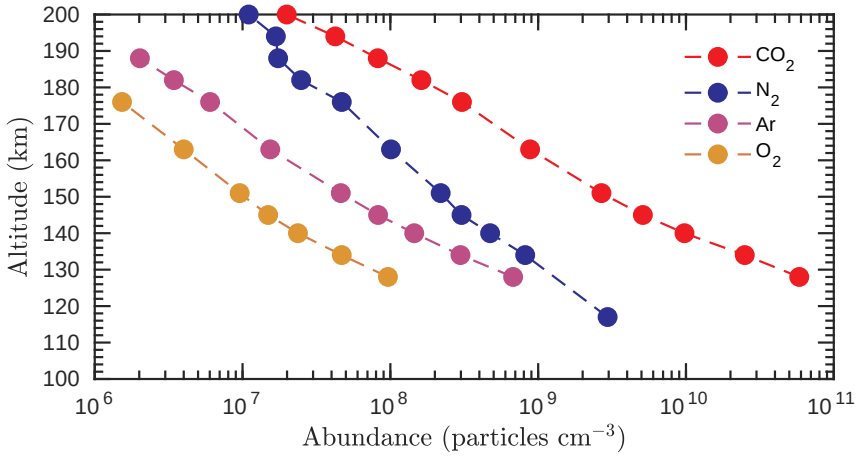

Fig 1. Neutral composition number density profiles in the thermosphere and exobase regions of the upper atmosphere of Mars measured by Viking 1 lander (Nier and McElroy, 1977). The lander covered solar zenith angles of 41–44° and ground coordinates in latitude and longitude of 14–17° and 302–306° respectively.

Table 1
Data availability sample; giving MOM orbit number and number of data files along with their time coverage.

Orbit no.	Observation start time	Observation end time	No. of files
31	17-10-2014 11:01	19-10-2014 18:43	28
32	20-10-2014 02:01	21-10-2014 06:38	10
34	28-10-2014 05:41	30-10-2014 20:32	16
35	01-11-2014 23:16	02-11-2014 14:01	4
36	02-11-2014 1626	05-11-2014 07:11	16
38	05-11-2014 10:13	08-11-2014 00:40	10
39	08-11-2014 0334	10-11-2014 18:08	12
40	11-11-2014 19:03	13-11-2014 11:57	10

differences in the variation of precipitable water (Davies, 1981; Jakosky and Farmer, 1982; Smith, 2009), role of recent degassing due to volcanic activity in the evolution of the modern atmosphere of Mars (Niles et al., 2010) and enhanced D/H (Deuterium/Hydrogen) ratio in the clay minerals pointing to a longer history of hydrogen escape and hence water (Mahaffy et al., 2015). The quadrupole mass spectrometer (QMS) as part of the instrument suite on the MSL's Curiosity rover measured the chemical concentrations and isotopic factions of volatile compounds. The surface atmospheric composition of Mars consists of about 96% carbon dioxide (CO_2) and small concentrations of nitrogen (N_2), argon (Ar), and trace amounts of oxygen (O_2), Water vapour (H_2O) and ozone (O_3) (Mahaffy et al., 2013). The complete set of near surface meteorological data obtained from Viking landers (1976) to the Curiosity rover (2012) have been analysed and results have been consolidated in terms of diurnal, seasonal and inter-annual variations of meteorological parameters including dust storms over a span of more than 20 Martian years (Martinez et al., 2017). A similar analysis to characterise the thermosphere-exosphere system has not been possible due to paucity of observational data building up time sequences of the altitude and latitudinal profiles of the meteorological parameters and neutral/ionised gas concentrations (Bougher et al., 2014).

Recently the Mars Orbiter Mission (MOM, 2014) and the Mars Atmosphere and Volatile Evolution (MAVEN, 2014) have been launched respectively by the Indian Space Research Organisation (ISRO) and the US Space Agency, NASA with the main purpose to have orbiting spacecraft gather continuous data on spatial (3-D) and temporal profiles of various atmospheric/ionospheric constituents, weather events including dust storms, existence and escape of hydrogen/water, interaction of solar wind plasma and electromagnetic phenomena and habitability aspects of Mars. The ExoMars mission has also been launched recently as a collaboration project between ESA and ROSCOSMOS and its Trace Gas Orbiter (TGO) is placed in a 400 × 400 km circular exospheric orbit for observing biologically relevant trace constituents such as methane (CH_4) and other organic gases (Olsen et al., 2017). From various instruments included in these three later missions, it is clear that the common objective has been to measure the trace gas constituents and their height profiles in the upper atmosphere of Mars. While, the measurements carried out by MOM and MAVEN were sensitive enough to include the upper thermosphere/exosphere altitudes, the TGO mission observed these constituents below about 100 km due to lower sensitivity. MAVEN makes additional observations of the constituents in the fringe of the mesosphere. The data obtained from these missions are being analysed by scientists all over the world and new insights into various phenomena are pouring in with a large number of research publications. Some of these, relevant to the present study, will be referred to in this report. However, it is an important point to note that till September 2014 when MOM and MAVEN arrived at Mars, the data from the Viking mission remained the only in-situ measurements of neutral and ion composition of the thermosphere and its fringe region just touching the exosphere of Mars.

The main purpose of this paper is to study the spatial and temporal distribution of atmospheric composition of the thermosphere-exosphere region of Mars which is essential to understand the diurnal, latitudinal, seasonal and solar activity driven variations and the escape of neutral/ion atmospheric species from Mars. The in-situ observations carried out by MENCA (Mars Exosphere Neutral Composition Analyser) and NGIMS (Neutral Gas and Ion Mass Spectrometer) on board MOM and MAVEN orbiter missions have opened up new vistas to further characterise the thermosphere-exosphere of Mars. The primary objective is therefore to reduce the gap in knowledge about the variations of atmospheric constituents in the exobase to exosphere of Mars using recent data from MENCA.

2. Early measurements of the upper atmosphere of Mars

The first in-situ observations providing the vertical profiles of neutral gases, ion, electron densities and temperatures of the atmosphere of Mars were carried out by the Viking-1 and Viking-2 landers when these descended down to the surface of Mars. The neutral mass spectrometric data on the composition of the upper atmosphere of Mars indicates that the main constituents of the Martian atmosphere are carbon dioxide (CO_2), Argon (Ar), molecular nitrogen (N_2), carbon monoxide (CO), and with photo-chemically produced atomic oxygen (O) (Nier and McElroy, 1977). The volume mixing ratios observed from Curiosity rover (MSL, 2012) for CO_2, Ar and N_2 are 0.960, 0.0193 and 0.0189, respectively (Mahaffy et al., 2013). The altitude variations of some important atmospheric constituents above the well mixed atmosphere, i.e., above the mesosphere and into the thermosphere, where the

Table 2
Sample records of combined total and partial pressures of H synchronised with UTC.

Time, UTC	Total pressure (torr)	Partial pressure (torr) for amu-1 (9-observed values)									Max. partial pressure (torr)
		1	2	3	4	5	6	7	8	9	
2014-12-16T11:15:58.729	1.20E-09	−1.30E-10	−1.00E-10	−1.00E-10	−9.60E-11	−1.20E-10	−1.20E-10	−1.20E-10	−1.10E-10	−1.10E-10	−9.60E-11
2014-12-16T11:16:10.947	1.70E-08	1.50E-10	2.60E-10	2.60E-10	2.70E-10	2.00E-10	1.40E-10	−4.70E-12	3.30E-11	8.50E-11	2.70E-10
2014-12-16T11:16:42.750	1.10E-08	3.70E-11	4.60E-11	5.20E-11	6.90E-11	4.40E-11	1.90E-12	1.60E-12	1.80E-12	1.50E-11	6.90E-11
2014-12-16T11:1700.998	1.00E-08	1.50E-11	1.40E-11	4.00E-11	2.90E-11	1.90E-11	2.00E-11	−1.40E-12	1.80E-11	5.00E-12	4.00E-11
2014-12-16T11:1721.172	9.90E-09	−9.40E-12	8.70E-12	2.30E-11	1.70E-11	3.10E-11	−6.20E-12	−1.80E-11	2.60E-12	7.40E-12	3.10E-11
2014-12-16T11:17:52.974	9.40E-09	9.30E-12	2.10E-11	2.80E-11	4.50E-11	2.20E-11	2.20E-11	−1.80E-11	3.90E-12	3.60E-12	4.50E-11
2014-12- 16T11:18:13.145	8.90E-09	−3.20E-11	4.30E-11	1.90E-11	3.50E-11	1.50E-13	3.30E-11	−6.50E-12	1.60E-11	-2.00E-11	4.30E-11
2014-12-16T11:1833.315	8.50E-09	−1.90E-11	1.10E-11	−2.10E-11	1.60E-11	−1.10E-11	2.00E-11	−2.40E-11	1.50E-12	2.10E-11	2.10E-11
2014-12-16T11:1903.197	8.30E-09	−1.40E-12	−5.30E-13	2.10E-11	1.70E-12	7.00E-13	8.70E-12	−1.90E-11	1.10E-11	1.60E-11	2.10E-11
2014-12- 16T11:1923.368	8.20E-09	−1.10E-11	−9.20E-12	2.70E-11	3.10E-11	−8.10E-12	7.20E-12	−1.20E-11	1.40E-11	1.10E-11	3.10E-11

diffusion of individual atmospheric species dominate in comparison to turbulent mixing (Haberle 1998), are shown in Fig. 1 as an example taken from Viking results (Nier and McElroy, 1977). During the period of atmospheric observation while in descent from 200 km, the lander covered solar zenith angles of 41–44° and ground coordinates in latitude and longitude of 14–17° and 302–306° respectively (Withers et al., 2002). So the data on altitude variation of the gaseous constituents shown in Fig. 1 are taken under similar solar radiation condition and within a marginal variation of 4° of latitude and longitude. These results were later extended from 200 to 300 km through scale height extrapolations (Hanson et al., 1977). After Viking, a number of orbiter, lander and rover missions have enriched our knowledge about Mars's atmospheric phenomena mainly in its meteorological context. Atmospheric model such as Mars Thermospheric General Circulation Model (MTGCM) (Bougher, 2012) and the Mars Climate Database (MCD) derived from models have been utilized to study the composition of Martian atmosphere extending into the exosphere. These results have been validated by using in-situ observations from Viking (Lewis et al., 1999) as well as observations carried out later by Mars Express (SPICAM - Spectroscopy for the Investigation of the Characteristics of the Atmosphere of Mars) and MAVEN (IUVS). Another advantage of MOM/MAVEN data is that it helps determining the solar activity effects as the observations have been taken during the period of moderately high solar activity condition as compared to Viking probe measurements.

The present work therefore involves conversion of the available near-raw data of MENCA experiment into a calibrated data set with associated tags of time, altitude, latitude, longitude and solar zenith angles for detailed analysis to derive the exospheric composition and its variability.

3. Creation of MENCA data set and method of analysis

The Indian Mars Orbiter Mission (MOM) was launched on 5 November 2013. The probe arrived in Mars on 24 September 2014 in an eccentric orbit of 422 km × 76,993 km with an orbital period of about 72 h. Later manoeuvres during December 2014 brought down the periareion altitude to around 262 km (Bhardwaj et al., 2016). One of the payload elements of MOM is MENCA for the measurement of total atmospheric pressure and partial pressures of various atmospheric constituents covering 1–100 atomic mass number (amu) units. MENCA is a quadrupole mass spectrometer consisting of an open ion source and a detector system which measures partial pressures of gas constituents with a mass resolution of 1 amu in a programmable range of 1–300 amu. It has two types of detectors, viz., Faraday Cup and a high gain Channel Electron Multiplier (CEM) providing a measurement sensitivity of $\sim 10^{-14}$ Torr with an uncertainty of ~15%. The instrument also has a Bayard Alpert gauge to measure the total pressure. The total pressure values are corrected in respect of any water contamination due to outgassing following the method of background subtraction. However, for this study the partial pressure values of water vapour and its likely products have not been used in the overall analysis. More details about the instrumentation, limitations, observation errors and sources of contamination have been discussed by Bhardwaj et al. (2015, 2016 with supporting information provided to the Journal by the authors). After one year of operation, the data from this experiment has been made available by the project for the period 24 September 2014 to 23 September 2015 through the ISRO Space Science Data Centre (ISSDC) website accessible from anywhere in the world. This archived data consists of total pressure and partial pressure values in the units of torr with time resolution of 12–30 s near periareion. Before this data can be used for scientific studies it needs further processing in terms of calibration factors and ancillary data like latitude, longitude, altitude and solar zenith angle.

The data is identified with respect to different orbit numbers of MOM for aforementioned period covering 88 orbits. The raw data of

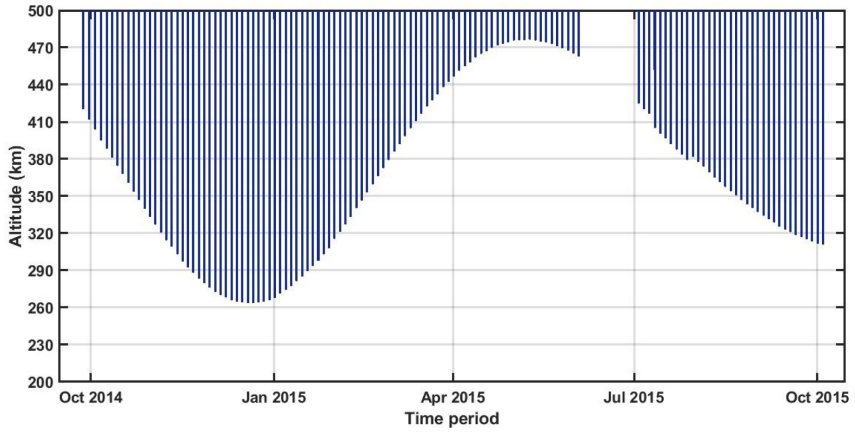

Fig 2. Periareion altitude coverage of MENCA observations during October 2014–October 2015.

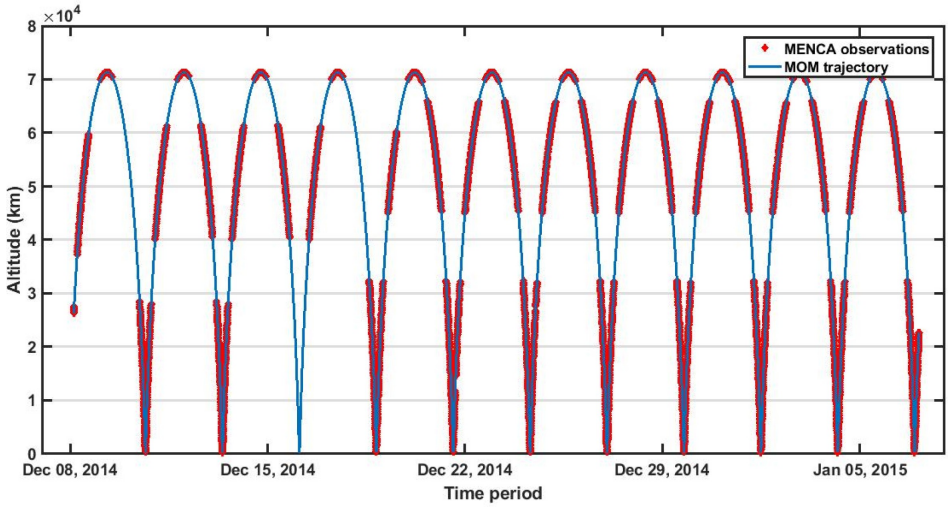

Fig 3. The MOM trajectories and MENCA observation periods in each orbit (darker lines) during December 2014.

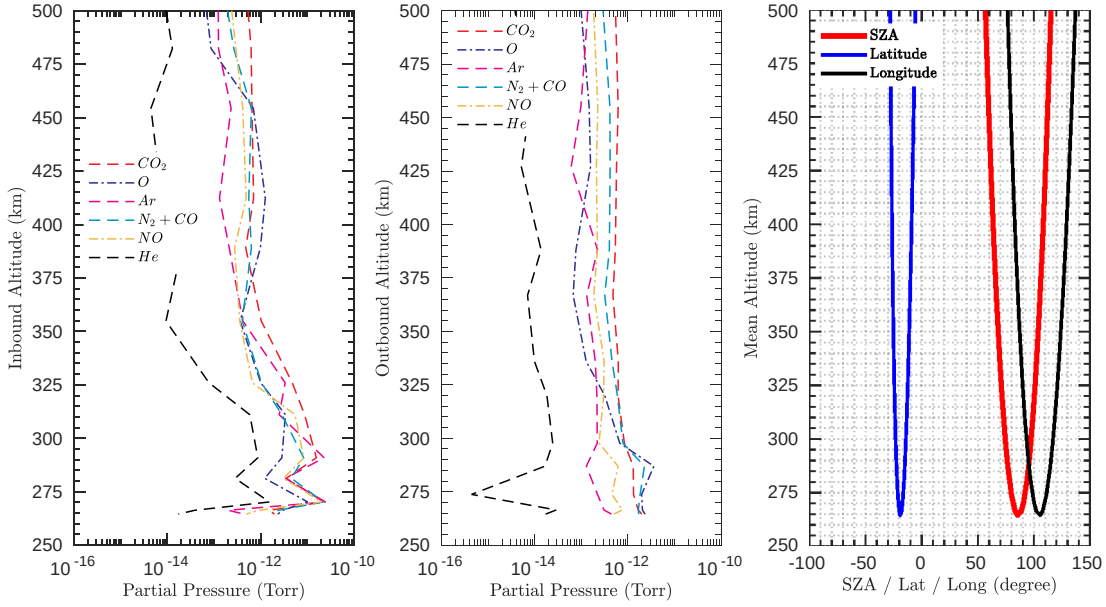

Fig 4. Partial pressures of exospheric constituents from MENCA observations related to MOM orbit No.55 (24 December 2014) shown for descending to periareion and ascending from periareion tracks separately. Also shown are the variations of solar zenith angle as MOM traces the path through the periareion and latitude/longitude coverage.

Table 3
Comparison of partial pressures ~260 km altitude from MENCA and Viking results.

Constituents (amu)	Partial pressure from MENCA		Partial pressure from Viking
	Torr	Pa	Pa
He (4)	4.18E-15	5.57E-13	–
N (14)	3.47E-13	4.63E-11	–
O (16)	7.03E-13	9.37E-11	1.90E-10
N_2 + CO (28)	6.89E-13	9.19E-11	2.09E-11
O_2 (32)	3.40E-13	4.54E-11	3.84E-13
Ar (40)	8.05E-14	1.07E-11	–
CO_2 (44)	9.31E-13	1.24E-10	7.24E-12
Total pressure	4.04E-12	5.38E-10	2.18E-10

each orbit is included in a number of file pairs, each pair containing the (a) total atmospheric pressure (in torr) and (b) partial pressures (in torr) of constituents for different time intervals. The individual files for partial pressures contain the data in a continuous time sequenced array form, which is converted into tabulated columnar format by marking each column for (i) time of observation in UTC, (ii) corresponding 9 values of partial pressures for each constituent between 1–100 amu and (iii) total pressures time synchronised with partial pressure measurement times using the second file in the pair. Table. 1 shows an example of information on number of files containing data in a streaming time sequence mode for different orbits.

ISSDC has also provided the specific SPICE (Spacecraft Planet Instrument C-matrix Events) kernel files for the one year period of observation consistent with the internationally standardised service modules (Acton, 1996; Acton et al., 2017) required to compute the altitude, latitude, longitude and solar zenith angle values tagged to each time of observation so as to characterise and tabulate the pressure data with respect to these localisation parameters.

Further data processing involves (a) combining each pair of files to convert into one file having the partial pressures (maximum pressure value out of 9 values of observation for each of the 100 amu bins) as well as the time synchronised total pressure. An example of such an arrangement is given in Table. 2, showing the 9 measurements of pressure values for the same time epoch and the selected maximum pressure value out of these nine values as most appropriate as given for atomic Hydrogen in the Table (the negative pressure values are rejected in iteration). Thus 100 maximum pressure values are selected between 1–100 amu for the same time epoch constituting a single record for further analysis, (b) computing the altitude, latitude, longitude and solar zenith angle for each time epoch of observation using the kernels of SPICE system mentioned earlier, (c) conversion of raw partial pressure data using calibration curves provided by the payload scientists (Das and Smitha, 2017) for different amu values. The final calibrated partial pressure values along with the associated ephemeral and spatial information for each orbit is used for further analysis and scientific studies of the atmospheric constituents of Mars.

After the above treatment of data, the MOM orbit-wise analysis is carried out to select the useful partial pressure values from the lowest altitude to about 600 km. This height limit is decided based on the requirement of our present study. The sum of the partial pressures of major gas constituents is also used to compute the total pressures for studying relative variation with time, altitude etc. This method is found useful when the concentrations of certain constituents like water vapour, molecular and atomic hydrogen etc. show abnormally high values due to degassing. Such contamination due to degassing has been reported by the payload group (Bhardwaj et al., 2017). Statistical analysis is carried out for deriving the monthly mean values and standard errors at 95% confidence interval.

4. Results

Preliminary results of MENCA measurements for a few selected MOM orbits during December 2014 have been published by the payload scientist's group (Bhardwaj et al., 2016, 2017) which provide some examples of exospheric composition profiles. The MENCA in-orbit payload operation plan was governed by the science objective to study the atmospheric composition in the exosphere which has been constrained by the variation of periareion (260–450 km) for the first year (October 2014–October 2015) of observation. Fig. 2 shows this variation of the altitude of the periareion of MOM spacecraft during the first year of data collection. The gaps in the orbital traces indicate that no MENCA observations were taken for about one month period of June–July 2015. During each MOM orbit the MENCA payload has been operated to cover the descending and ascending tracks near the periareion as well as at locations away from the periareion mainly to serve as background information or the noise level of the experiment. Fig. 3 shows the MOM tracks for the 11 orbits during December 2014 with the MENCA observation periods indicated by darker lines along these tracks. It can be seen that the observations have been taken at different

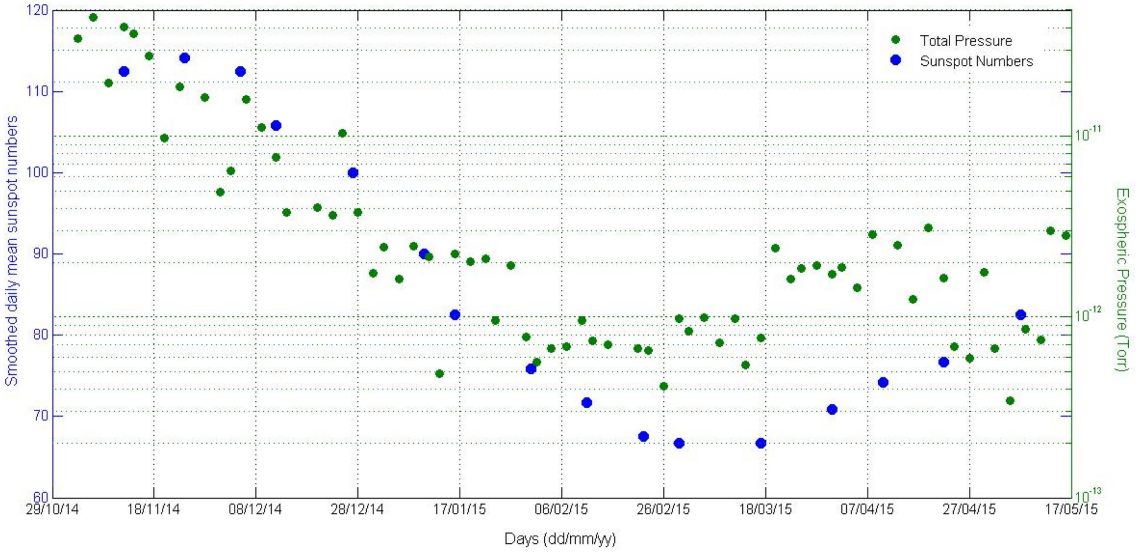

Fig 5. Variation of total pressure estimated by summing partial pressures of a number of constituents for the minimum altitude of each MOM orbit #28 to #107 and smoothed daily mean sunspot numbers (SSN) during the period Oct 2014–May 2015. The correlation coefficient (r) between the two parameters is 0.76.

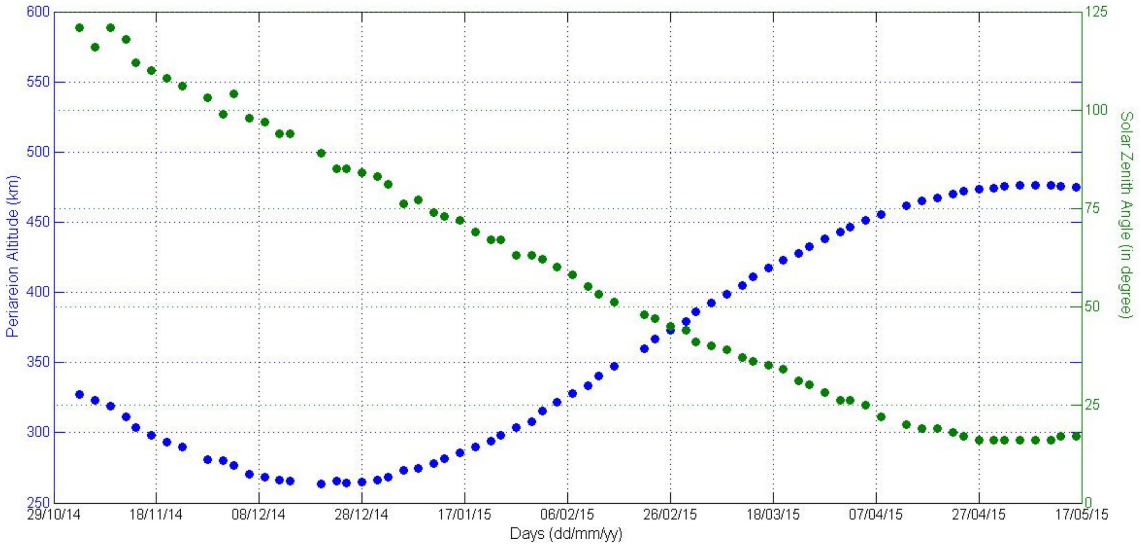

Fig 6. Variation of periareion altitude for each MOM orbit #28 to #107 along with the corresponding solar zenith angles during the period Oct 2014–May 2015. The correlation coefficients (r) between the total pressure and these two parameters (periareion altitude and zenith angle) are −0.36 and 0.39 respectively. .

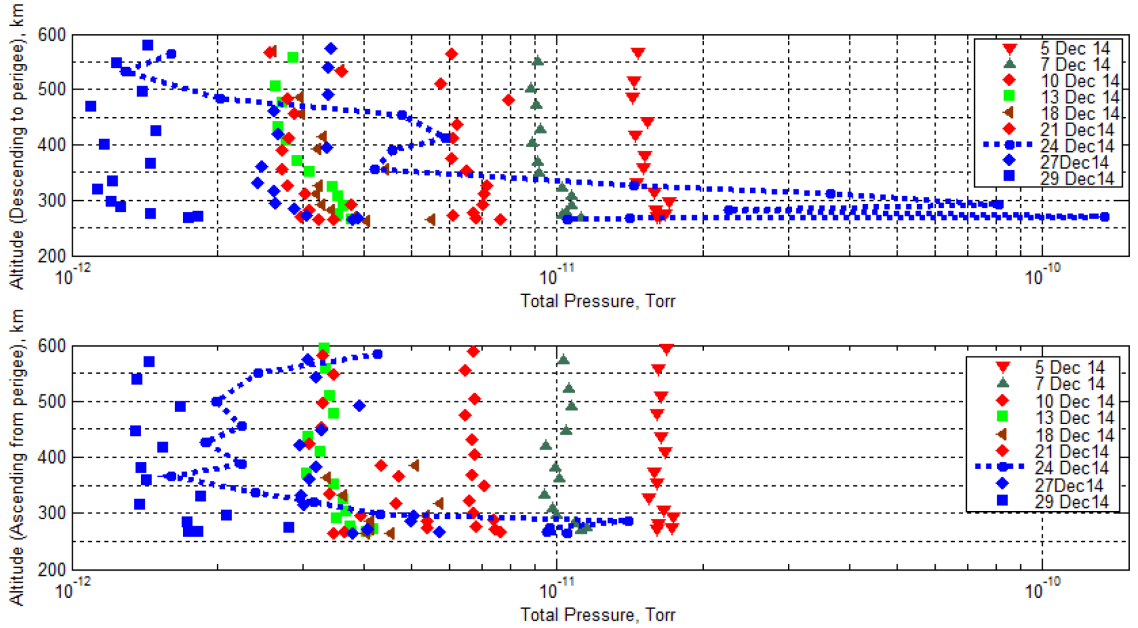

Fig 7. Vertical profiles of total pressure (derived as per method mentioned in this paper) for the descending and ascending part of MOM orbits during December 2014.

sections of the track ensuring the altitudes near the periareion of MOM for observing the exosphere of Mars starting from about 260 km altitude. This height coverage of composition data is unique as there have been hardly any such in-situ measurements of Martian upper atmosphere deep into the exosphere.

The in-orbit mass spectrometric observations of MENCA payload are linked to the planetary coordinates in terms of altitude, latitude, longitude and solar zenith angle. These are determined using the auxiliary data files provided along with the pressure data of the atmospheric constituents.

The MENCA dataset generated following the above procedure has been analysed mainly to study the variation of partial pressures of gaseous composition. The exospheric profiles of these parameters are obtained for individual orbits specifically covering the region around periareion of MOM. A typical example of the altitude profiles of exospheric constituents derived from MENCA observations of the orbit no. 54 for descending and ascending tracks of MOM is shown in Fig. 4. Here we notice that pressure values drop with altitude by about 2 orders of magnitude between 260 and 530 km for descending track. However for the ascending part of orbit (a) the gradient is slower particularly between 260–350 km and (b) the absolute magnitude of this reduction in pressure is lower between 260 and 350 km when sun went down below the horizon as evident from the variation of SZA shown in the same figure. Combined together this decrease of pressure is slower with altitude compared to the Viking results below ~200 km due to the difference that above the thermosphere the gaseous elements follow diffusion equilibrium paths which are different for different species depending on their mass and temperature. It can also be seen that in the region of exosphere above 300 km, CO_2, N_2, O and O_2 are the dominant atmospheric constituents. The figure also shows considerable reduction in atomic oxygen (O) density after sunset. This is because O is mainly a product of photodissociation of O_2 and CO_2. As it is not possible to

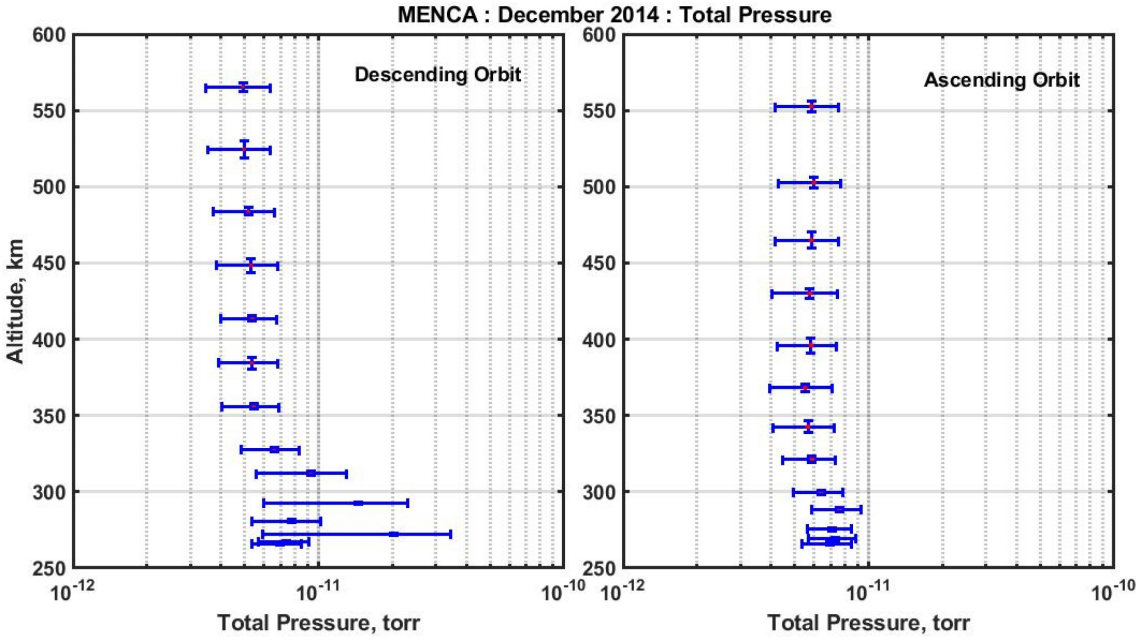

Fig 8. Mean total pressure profiles with standard errors derived from all the measurements during December 2014 both for ascending and descending parts of the orbits.

separate N_2 and CO having the same amu of 28, the effective value of N_2 would be less due to the contribution of CO which is a photo-dissociation product of CO_2 (Bhardwaj et al., 2017).

The partial pressure measurement mentioned above have also been compared with similar measurements carried out earlier during Viking mission. Table. 3 provides the pressure values in torr and pascal for different atmospheric constituents and a typical comparison from earlier measurements of Viking as derived by Hanson et al. (1977). The comparison shows that the partial pressure values generally are of the same order.

For further analysis, we consider CO_2, O, N_2 and Ar as the main elements to study the variation of exospheric composition. Also the total pressure is computed by summing up the partial pressures of all the major constituents as CO_2, O, N_2, CO, NO, O_2, Ar, N and He. The contribution due to water vapour (H_2O), H_2 and H are excluded from the sum as these constituents may be modulated by the degassing of the spacecraft.

An integrated study has been carried out to determine the variation of total pressure around the periareion altitudes of MOM spacecraft during the period from October 2014 to May 2015 covering the orbit numbers 28–107 and these results are shown in Figs. 5 and 6. It can be seen that the total pressure values at the minimum altitudes (perireion) of different orbits vary with time and this is broadly in agreement with the total pressure values decreasing with increasing altitude of the observation.

However, a more striking feature (Fig. 5) is the clear association of temporal variation of the total pressure with the time series of the smoothed daily mean sunspot numbers (SSN). The SSN parameter is computed using individual daily mean values obtained from the World Data Centre (WDC), Belgium. The solar zenith angle variation during the same period shown in Fig. 6 does not have any significant effect on the pressure values as compared to the solar activity control of the variations for these altitudes. These results are also substantiated by computing the correlation coefficients mentioned in the captions of Figs. 5 and 6. The correlation coefficient of 0.76 between total pressure and solar activity shows a very strong association between the two parameters. The other two correlation coefficients of total pressure with altitude and solar zenith angle are very weak with the values of -0.36 and 0.39 respectively. The result points to the fact that the solar activity control of the distribution of composition measured in terms of total pressure is a dominant factor in addition to the scale height dependant exponential decrease of the pressure due to constituents' density being in a diffusion intensive exospheric region above ~200 km. The phenomena related to solar activity would produce heating due to absorption of solar UV radiation resulting in photo-dissociation and photo-ionisation. As a secondary effect the energetic lighter constituents may be lost due to Jeans and pick-up ion escapes.

The total pressure profiles for exospheric altitudes have been estimated from the available data per orbit and the results for both descending and ascending tracks are shown for the month of December 2014 in Fig. 7. It can be seen that, except for the anomalous pressure values on 24 December 2014 (reasons explained later in this paper), there is a progressive decrease in total pressure at all altitudes from beginning to end of the month and this decrease correlates well with the decrease in the smoothed daily mean SSN mentioned earlier. The large reduction of the total pressure within a month is difficult to explain without invoking the solar activity effects. By checking the variations of solar zenith angles, latitude and longitude, it is found that the effect of these is at best very marginal and not effective in bringing a change of this magnitude within a period of one month for these altitudes. The changes in solar UV/X-ray fluxes arriving at Mars due to variations of solar activity have a strong modulating effect on exospheric pressures. These variations due to solar activity are found to be larger than the standard errors at 95% confidence interval for both descending and ascending orbital paths as shown in Fig. 8. Where the standard error of the means at 95% confidence interval is given by $m \pm (1.96\sigma/\sqrt{n})$, where m is the sample mean, σ - the standard deviation of mean and n - the number of samples. These error bars are shown in the figure.

Only at two points between 250–300 km altitude for the descending track of the orbit the error bars are relatively large due to the anomalous pressures profile of 24 December 2014. This point is addressed again later in this paper. Similar analysis is carried out separately for the partial pressures of CO_2 and O by taking the mean pressure and altitude values of descending and ascending part of the orbital tracks. Fig. 9 shows the individual days profiles of CO_2 and O pressures for different days (pertaining to different orbit numbers) of December 2014. From this figure the following points can be noted: (a) there is a considerable day to day variability of the altitude profiles of both CO_2

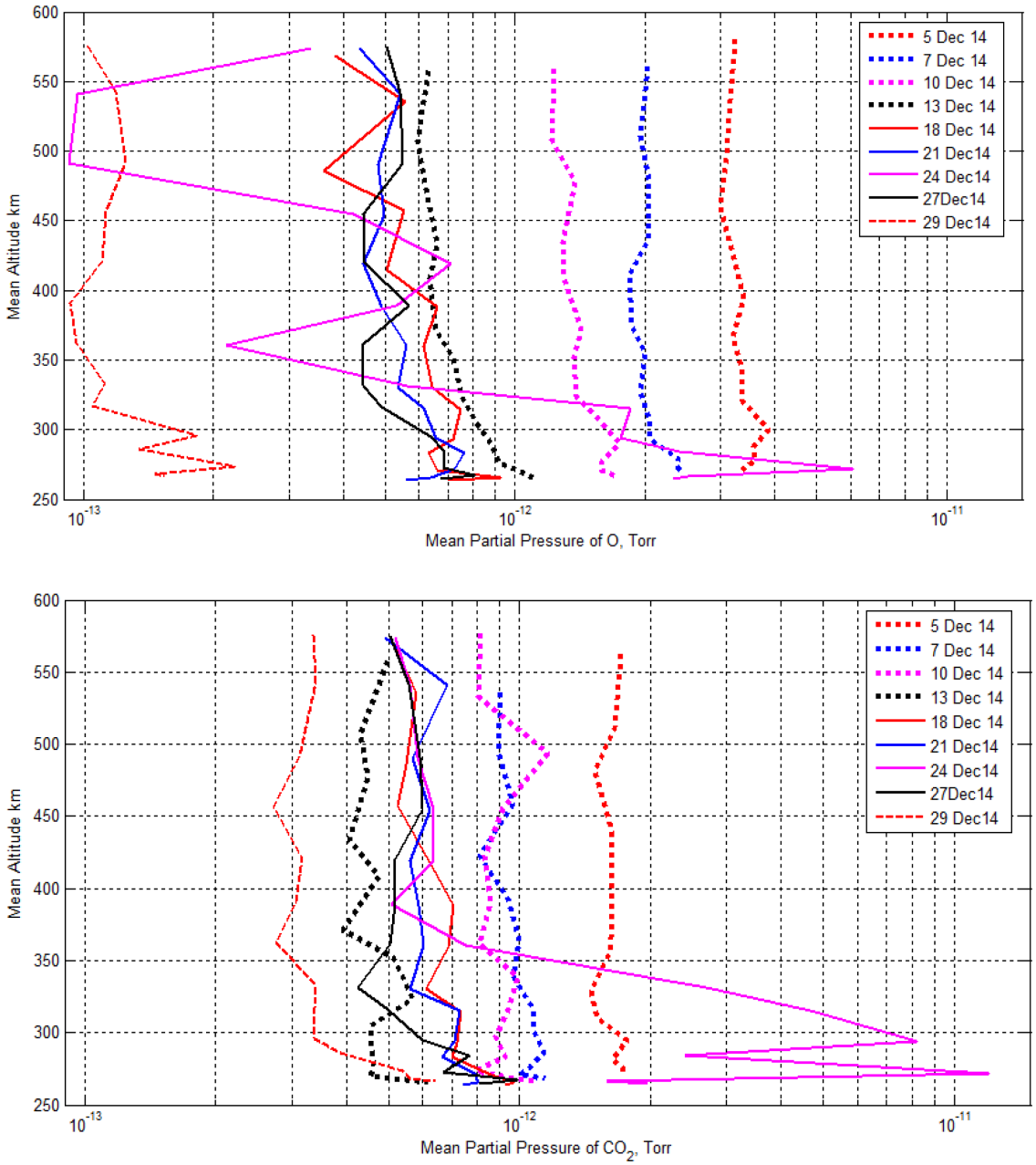

Fig 9. MOM Orbit wise vertical profiles of partial pressure of CO_2 (top panel) and O (bottom panel) measured during December 2014.

and O with a consistent decrease of pressure at all atitudes with respect to advancing days in the period, (b) the O pressure is generally higher than that of CO_2 before the anomalous event of 24 December, (c) On 24 December there is a large enhancement of CO_2 and O pressures between 260–350 km when the solar proton fluxes are enhanced due to a moderate Coronal Mass Ejection (CME) event in progress during 20–25 December 2014, (d) the anomalous pressure values of CO_2 are higher than that of O at all altitudes and the O pressures are lower compared to CO_2 pressures while recovering from the event after 24 December 2014.

In order to explore the anomalous pressure enhancements of CO_2 and O, contours of these pressures with respect to time and altitude are plotted for periods between 21–27 December and 18–27 December as shown in Fig. 10(a) and (b), respectively. These figures depict the following (a) CO_2 pressures started increasing anomalously from 22 Dec and reached 2 peaks by 24 Dec one around 275 km and the other around 295 km, (b) atomic oxygen (O) started increasing from 19 Dec and reached one strong peak around 275 km between 22–23 Dec, (c) the height range of the effect of pressure increase for CO_2 continued above 360 km but for O it tapered around 330 km.

As can be inferred from the results presented in Fig. 5, these anomalous effects are to be examined in terms of any eruptive events of solar high energy electromagnetic and charged particle radiations during December-2014 as both these radiations would arrive at Mars and interact with its atmosphere and surface. Since Mars does not have a magnetic field like that of Earth, in addition to the UV/X-rays, the charged particles or solar plasma components like energetic protons would directly interact with the neutral composition and initiate photodissociation and photoionisation. The absorption of particle energy would also result in modified densities of atmospheric species in certain height ranges due to increase in temperatures. To check this phenomenon, the solar activity as revealed by the smoothed daily mean SSN mentioned earlier, and the solar proton densities measured by Advanced Composition Explorer (ACE) spacecraft (Srl.caltech.edu, 2018) are plotted for the month of December 2014 and shown in Fig. 11. The

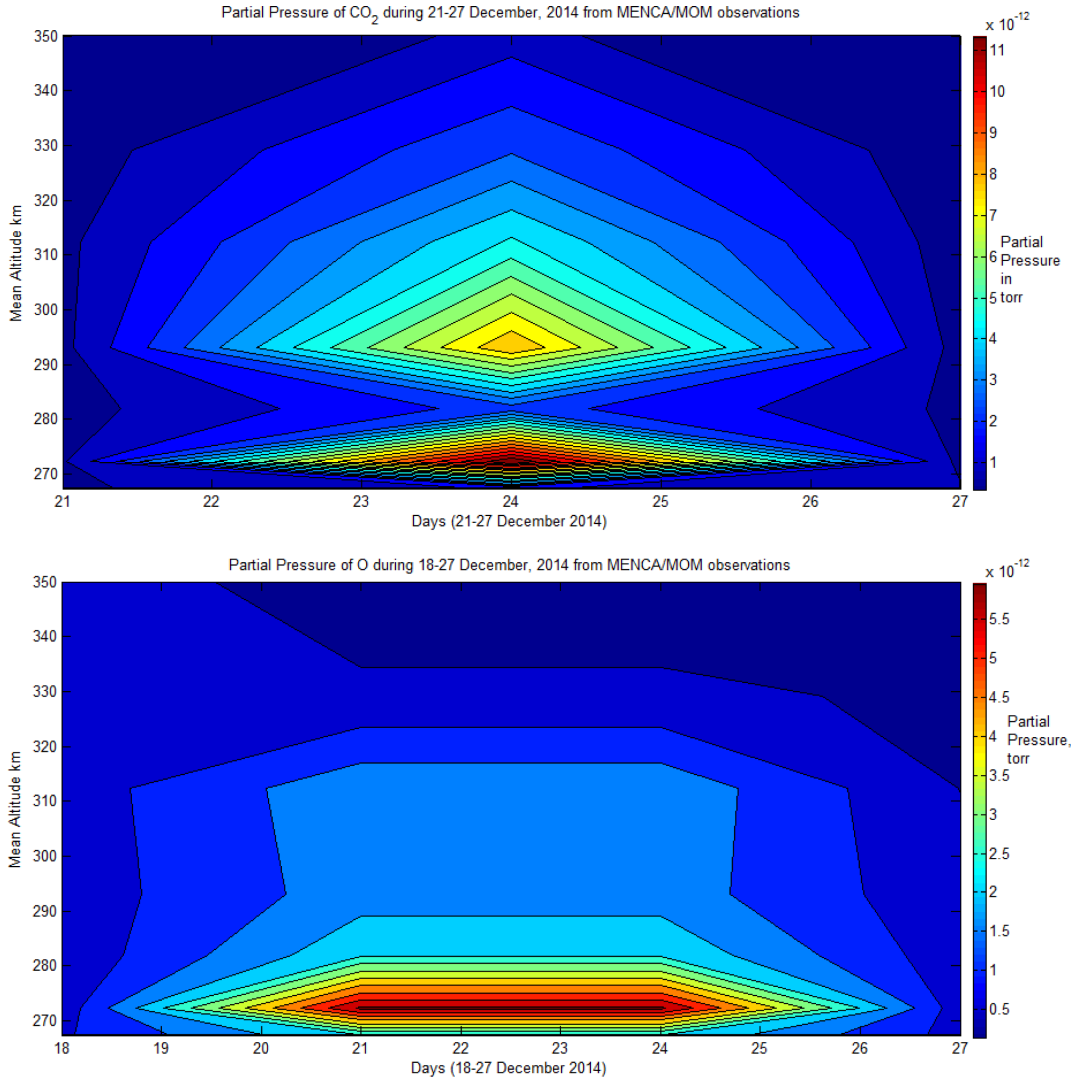

Fig 10. (a) Partial pressure contours of CO_2 during 21–27 Dec, 2014 (upper panel) and (b) partial pressure contours of O during 18–27 Dec, 2014 from MENCA/MOM observations.

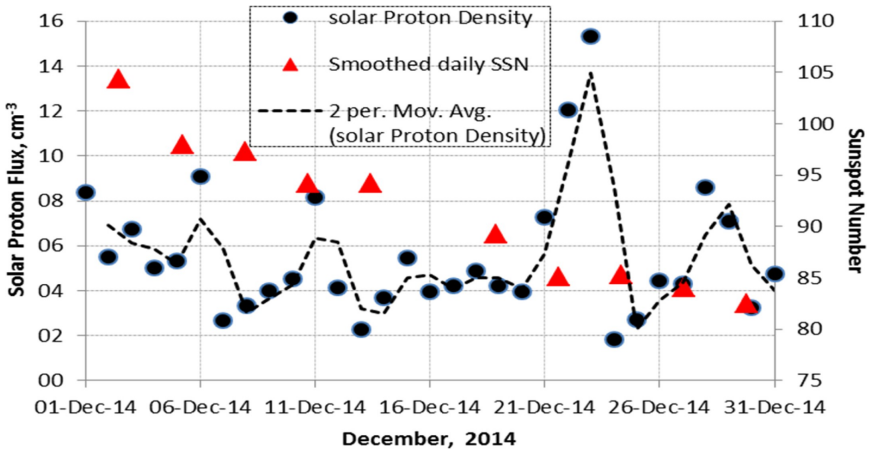

Fig 11. Variation of daily mean (smoothed) sunspot numbersand solar proton flux (with moving averages) during December 2014.

UV/X-rays fluxes for the period did not show any occurrence of solar flare during this period and hence are not shown in the figure. While it is known that CMEs, in large number of cases, are preceded by solar flares, it is also shown that this may not always be the case and occurrence of moderately strong CMEs during a very low solar activity year of 2009 has occurred without any associated solar flare (Nagaraja et al., 2018). Hence the variation of solar proton fluxes along with their moving averages in Fig. 11 indicates that there is a large increase of energetic proton fluxes during the period 21–26 Dec, 2018 with peak fluxes around 23 Dec, 2014. The exact date of the peak of the

corresponding CO2 and O pressures is not accurately discernable due to the fact that the observation periodicity is restricted to about 3 days orbital period of MOM. However it is clear the peaks of enhanced pressures of CO2 has occurred with a delay of about 1–1.5 days. The O pressures on the other hand show a broad maximum. The density of O depends, apart ftom temperature on the photolysis and photoionisation effects and hence its enhancement and persistence of its peak values is primarily a cumulative effect compared to that of CO_2.

5. Conclusion

- MENCA data available from ISSDC in its nearly raw form has been processed to create a new data set with orbit-wise data assimilation particularly between 250 and 600 km for the period from September 2014 to September 2015. The ancillary information on the altitude, latitude, longitude and solar zenith angles obtained using the SPICE kernels have been tagged to each epoch of time and measurement. Also the partial pressures of the exospheric constituents of Mars have been converted to actual values using the calibration curves and normalisation procedure.
- As a sample of altitude-pressure profiles of exospheric constituents CO_2, O, ($N_2 + CO$), O_2, NO, He & Ar obtained from MOM orbit No. 55 near the periareion (covering ~262–600 km in the exosphere of Mars) are generated and presented using this data set. The variation of profiles generally follows the exponential decrease with altitude with atomic Oxygen (O) concentrations being larger than that of CO_2 during daylight hours.
- The total pressure is computed by summing up the partial pressures of all the major constituents i.e., CO_2, O, N_2, CO, NO, O_2, Ar, N & He to ensure removing those constituents affected by the degassing of water vapour. The variation of the total pressure at the periareion altitudes during October 2014 - May 2015 shows a strong correlation with the smoothed daily mean sunspot numbers.
- A time series plot of partial pressure-altitude profiles of CO_2 and O during December 2014 shows gradual decrease in partial pressure values (at all altitudes) from beginning to end of December that is again consistent with the decrease in the smoothed daily SSN.
- Superimposed on the December 2014 profiles of partial pressures of CO_2 and O, there are anomalously high-pressure profiles of both CO_2 and O peaking on 24 December 2014. The contour plots show more details of the temporal and altitude build up, the peak and recovery phases of this anomaly. It is found that this anomaly is due to a moderately strong CME event of Sun leading to the enhanced radiation near Mars which peaked around 23 December 2014.

Acknowledgement

Authors are grateful to Indian Space Research Organisation (ISRO) for providing necessary funds to carry out this work under a research project vide ref: ISRO: SPL:01.01.33/16. We acknowledge the use of data from MENCA of MOM, first Mars mission of the ISRO, archived at the Indian Space Science Data Centre (ISSDC). Thanks are also due to Dr Anil Bhardwaj, Payload-PI, MENCA-MOM, and MENCA scientific group, SPL, VSSC for valuable inputs and discussion.

Supplementary material

Supplementary material associated with this article can be found, in the online version, at doi:10.1016/j.newast.2019.101349.

References

Acton, C.H., 1996. Ancillary data services of NASA's navigation and ancillary information facility. Planet. Space Sci. 44 (1), 65–70.
Acton, C.H., Bachman, Nathaniel, Semenov, Boris, Wright, Edward, 2017. A Look Toward the Future in the Handling of Space Science Mission Geometry. Planetary and Space Sciencehttps://doi.org/10.1016/j.pss.2017.02.013.
Acuna, M.H., et al., 1999. Global distribution of crustal magnetization discovered by the Mars global surveyor MAG/ER experiment. Science 284, 790–793. https://doi.org/10.1126/science.284.5415.790. 5415.
Barabash, S., Fedorov, A., Lundin, R., Sauvaud, J.A., 2007. Martian atmospheric erosion rates. Science 315, 501–503. https://doi.org/10.1126/science.1134358. 5811.
Barker, E.S., 1972. Detection of molecular oxygen in the Martian atmosphere. Nature 238, 447–448.
Barth, C.A., Dick, M.L., 1974. Ozone and polar hood on Mars. Icarus 22 pp. 205-201.
Bhardwaj, 2015. MENCA experiment aboard India's Mars Orbiter Mission. Curr. Sci. 109 (6), 1106–1113. https://doi.org/10.18520/v109/i6/1106-1113.
Bhardwaj, 2017. Observation of suprathermal argon in the exosphere of Mars. Geophys. Res. Lett. 44, 1–8. https://doi.org/10.1002/2016GL072001.
Bhardwaj, 2016. On the evening time exosphere of Mars: result from MENCA aboard Mars orbiter mission. Geophys. Res. Lett. 43, 1862–1867. https://doi.org/10.1002/2016GL067707.
Bougher, S.W., Cravens, T.E., Grebowsky, J., Luhmann, J., 2014. The aeronomy of Mars: characterization by MAVEN of the upper atmosphere reservoir that regulates volatile escape. Space Sci. Rev. https://doi.org/10.1007/s11214-014-0053-7.
Bougher, S.W., Aug 2012. JPL/CDP report. pp. 1–9.
Carleton, N.P., Traub, W.A., 1972. Detection of molecular oxygen on mars. Science 177, 988–992.
Das, T.P., Smitha V, T., April 2017. Space Physics Laboratory 6 Vikram Sarabhai Space Centre, Thiruvananthapuram, India Private Communication.
Davies, D., 1981. The Mars water cycle. Icarus 45, 398–414. https://doi.org/10.1016/0019-1035(81)90043-9.
Haberle, R.M., 1998. Early Mars climate models. J. Geophys. Res. 103 (E12), 28467–28479. https://doi.org/10.1029/98JE01396.
Hanson, W.B., Sanatani, S., Zuccaro, D., 1977. The Martian ionosphere as observed by the Viking retarding potential analyzers. J. Geophys. Res. 82 (28), 4351–4363. https://doi.org/10.1029/JS082i028p04351.
Hanson, W.B., Mantas, G.P., 1988. Viking electron temperature measurements: evidence for a magnetic field in the Martian ionosphere. J. Geophys. Res. 93 (A7), 7538–7544. https://doi.org/10.1029/JA093iA07p07538.
Jakosky, B.M., Farmer, C.B., 1982. The seasonal and global behavior of water vapor in the Mars atmosphere—Complete global results of the Viking atmospheric water detector experiment. JGRP 87, 2999–3019.
Nagaraja, Kamsali, Praveen Kumar, B., Chakravarty, S.C., 2018. X-ray flares and coronal mass ejections (CMEs) during very quiet solar activity conditions of 2009. Ind. J. Pure Appl. Phys. 50, 621–623.
Kaplan, L.D., Connes, J., Cannes, P., 1969. Carbon Monoxide in the Mars Atmosphere. Astrophys.J. 157, LI87–L192.
Lane, A.L., Barth, C.A., Hord, C.W., Stewart, A.I., 1973. Mariner 9 ultraviolet spectrometer experiment: observations of Ozone on Mars. Icarus 10, 102–l08.
Lewis, S.R., Collins, M., Read, P.L., 1999. A climate database for Mars. J. Geophys. Res. 104 (E10), 24.
Magalhaes, J.A., Schofield, J.T., Seiff, A., 1999. Results of the Mars pathfinder atmospheric structure investigation. J. Geophys. Res. 104, 8943–8956.
Mahaffy, P.R., et al., 2015. The imprint of atmospheric evolution in the D/H of hesperian clay minerals on Mars. Science 347, 412–414.
Mangold, N., C. Quantin, V. Ansan, C. Delacourt, P. Allemand, Evidence for precipitation on Mars from dendritic valleys in the valles marineris area, Science, 305, pp. 78–81, 2004.
Martinez, G.M., et al., 2017. The modern near-surface Martian climate: a review of in-situ meteorological data from Viking to curiosity. Space sci. rev. https://doi.org/10.1007/s11214-017-0360-x.
Moroz, V.I., 1998. Chemical composition of the atmosphere of Mars. Adv. Space Res. 22 (3), 449457.
Nier, A.O., McElroy, M.B., 1977. Composition and structure of Mars' upper Atmosphere- results from the neutral mass spectrometers on Viking 1 and 2. J. Geophys. Res. 82, 4341–4349.
Niles, P.B., W. Boynton, J.H. Hoffman, D.W. Ming, D. Hamara, Science, 329, pp. 1334–1337, 2010.
Olsen, K., Montmessin, Franck, Fedorova, A., Trokhimovskiy, Alexander, Korablev., Oleg, 2017. Trace gas retrievals for the exomars trace gas orbiter atmospheric chemistry suite mid-infrared solar occultation spectrometer. In: European Planetary Science Congress 2017, Sep 2017. Riga, Latvia. 11 EPSC2017-938.
Owen, T.S., Biemann, K., Rusbneck, D.R., Biller, J.E., Homarth, D.W., Lafleur, A.L., 1977. The composition of the atmosphere at the surface of Mars. J. Geophys. Res. 82, 4635–4639.
Mahaffy, P.R., et al., 2013. Abundance and isotopic composition of gases in the Martian atmosphere from the curiosity rover. Science 341, 263.
Withers, P., Lorenz, R.D., Neumann, G.A., 2002. Comparison of Viking lander descent data and mola topography reveals kilometre-scale offset in Mars atmosphere profiles. Icarus 159, 259–261. https://doi.org/10.1006/icar.2002.6914.
Sagdeev, R.Z., Zakharov, A.V., 1989. Brief history of the phobos mission. Nature 341 (6243), 581–585. https://doi.org/10.1038/341581a0.
Smith, M.D., 2009. THEMIS observations of Mars aerosol optical depth from 2002–2008. Icarus 202, 444–452.
Squyres, S.W., et al., 2006. Overview of the opportunity mars exploration rover mission to meridiani plannum: eagle crater to purgatory ripple. J. Geophys. Res. 111, E12S12.
Srl.caltech.edu, ACE Mission available athttp://www.srl.caltech.edu/ACE/ASC/level2/swepam_l2desc.html, 2018.
Young, L.D.G., Young, A.T., 1977. Interpretation of high-resolution spectra of Mars. IV. new calculations of CO abundance. Icarus 30, 75–79.